Romanian Reports in Physics **71**, 903 (2019)

DYNAMICS OF THE PULSEJET ENGINE IN VERTICAL MOTION WITH LINEAR DRAG

MIRCEA DOLINEANU, TIBERIUS O. CHECHE*

University of Bucharest, Faculty of Physics, P.O. Box MG-11, RO-077125, Bucharest, Romania
E-mails: *mircea_dolineanu@yahoo.com*
*Corresponding author: *tcheche@brahms.fizica.unibuc.ro*

Received August 2, 2018

Abstract. The momentum conservation law is applied to analyse the kinematics of pulsejet equipped systems in vertical motion in a uniform gravitational field in the presence of linear drag. The model is applied to jetting paralarvae moving in sea water in vertical direction.

Key words: momentum conservation, laminar flow, biomechanics movement.

1. INTRODUCTION

In physics, the conservation laws play a major role in describing the motion. For example, in the case of more complicated motion involving collisions of a gravitational pendulum [1] or in the more complex motion of the rigid body [2] or quantum particles [3, 4, 5, 6] or nucleation [7], the momentum, angular momentum and energy are physical quantities of crucial importance which obey conservation laws. The systems that generate reaction thrust through an intake/exhaust cycle are widely spread in the nature and technology; some cephalopods or aircrafts equipped with pulsejet engine are such examples. The processes which take place in such engines are complex and constitute a direction of research in the naval or aerospace engineering. The pulsejet engine works by consuming energy in a cyclic process in which a fluid amount is taken from the environment and then expelled at a high relative velocity back to the environment. The cycle is named pulse. For the mentioned examples, the energy is obtained by the locomotive system of the animals or by fuel ignition in the aircrafts. Modelling the reaction thrust of such propeller is a complex task and introducing an easier to handle model of reasonable accuracy is, from both pedagogic and research perspective, useful. Previous works on reactive engines demonstrate that the momentum conservation is a physical law of primary importance in explaining the dynamics of such systems. For example, in [8] the momentum conservation is applied to estimate the performance of a staged rocket as function of its fuel properties, whereas in [9] the speed behavior of the Space Shuttle during its first two minutes of flight from liftoff is analyzed from a didactical

point of view. In [10], the momentum conservation law is applied to analyze the kinematics of a pulsejet engine in vertical motion in a uniform gravitational field in the absence of friction. In this work, we extend the model introduced in [10, 11] and, using the momentum conservation, we explain the kinematics of the pulsejet equipped systems (PES) in presence of drag. When modelling squid, the intake and exhaust are thought as being short comparatively to the time interval between two consecutive pulses [12, 13]. For a simpler modelling we approximate the intake/ exhaust cycle as being instantaneous comparatively to the pulse period. Also we consider the PES is moving in vertical direction in uniform gravitational field with linear drag and the pulse is periodic. Such model is attractive because, as it will be shown, it provides analytical and semi-analytical results easy to interpret.

The structure of the paper is as follows. In section 2, we present the theoretical model which describes the dynamics of the pulsejet in vertical motion in presence of linear drag. Relevant (critical) periods of the pulses are discussed and compared for a check with the results from the literature for the motion in absence of friction. In section 3, the theory is applied to simulate motion of some paralarva meso-plankton experiencing linear drag. In the last section we present our conclusions.

2. DYNAMICS OF PULSEJET VERTICAL MOTION IN PRESENCE OF LINEAR DRAG

First, we describe the dynamics of the ballistic vertical motion. The drag force is proportional with the velocity,

$$\mathbf{F}_r = -k\mathbf{v}, \quad k > 0, \tag{1}$$

and according to the Newton's second law for the vertical motion on an upward oriented y axis, we have

$$M\ddot{y} = -kv - Mg, \tag{2}$$

where M is the mass of the PES and $\dot{y} = v$ and g is the magnitude of the gravitational field. Integration of eq. (2) with the initial conditions $\dot{y}(0) = v_0$ and $y(0) = y_0$ is immediate and one obtains

$$v = \left(v_0 + \frac{g}{\gamma} \right) e^{-\gamma t} - \frac{g}{\gamma}, \tag{3a}$$

$$y = \frac{1}{\gamma} \left(v_0 + \frac{g}{\gamma} \right) \left(1 - e^{-\gamma t} \right) - \frac{gt}{\gamma}, \tag{3b}$$

where $\gamma = k/M$.

Second, by using the momentum conservation law as exposed in [10], we describe the dynamics of the PES in vertical motion in presence of linear drag. Thus, denoting by u the speed (with respect to the PES) of the exhausted amount m of fluid, from momentum conservation law, after the first pulse, with respect to the laboratory frame (LF), the PES has the speed

$$V_0 = fu, \tag{4}$$

where $f = m / M$ and V_0 is the magnitude of the PES velocity (the PES moves in opposite direction to the gravitational field). Then, the motion is described by a 3-stage process series of *vertical ballistic motion + intake + exhaust*. Thus, until the second pulse, the PES ballistically moves in the time interval $(0, \tau)$ (with τ the period of the pulses) under the laws expressed by eqs. (3a, b) and just before the second pulse we have

$$V_1^0 = \left(V_0 + \frac{g}{\gamma}\right)e^{-\gamma\tau} - \frac{g}{\gamma}, \tag{5a}$$

$$Y_1 = \frac{1}{\gamma}\left(V_0 + \frac{g}{\gamma}\right)\left(1 - e^{-\gamma\tau}\right) - \frac{g\tau}{\gamma}, \tag{5b}$$

where we considered the starting position is the origin of the LF. For the intake process the momentum conservation is written as,

$$MV_1^0 = (m + M)V_1^1, \tag{6}$$

where V_1^1 is the velocity just after the second intake (at $t = \tau$) in the LF. For the exhaust process the momentum conservation is written as,

$$(m + M)V_1^1 = MV_1 + m(-u + V_1^1), \tag{7}$$

where V_1 is the velocity just after the second exhaust in the LF. From Eqs. (5–7), one obtains that the velocity just after the second pulse is

$$V_1 = \frac{V_1^0}{1 + f} + fu, \tag{8}$$

and the position just after the second pulse is

$$H_1 = \frac{1}{\gamma}\left(V_0 + \frac{g}{\gamma}\right)\left(1 - e^{-\gamma\tau}\right) - \frac{g\tau}{\gamma}. \tag{9}$$

The motion continues from position H_1 with the launch velocity V_1 and a new 3-stage process of vertical ballistic motion + intake + exhaust. Generalizing, the velocity (with respect to the LF) recurrence is given by,

$$V_n = \frac{1}{1+f}\left[\left(V_{n-1} + \frac{g}{\gamma}\right)e^{-\gamma\tau} - \frac{g}{\gamma}\right] + fu, \quad V_0 = fu, \tag{10}$$

and the position recurrence is given by,

$$H_n = H_{n-1} + Y_n, \quad Y_n = \frac{1}{\gamma}\left(V_{n-1} + \frac{g}{\gamma}\right)\left(1 - e^{-\gamma\tau}\right) - \frac{g\tau}{\gamma}, \quad H_0 = 0, \tag{11}$$

where V_n and H_n are the velocity and position just after the $(n+1)^{\text{th}}$ pulse. In eq. (11), Y_n is obtained by using the form from Eq. (5b). The solution of the recurrences from Eqs. (10) and (11) is as follows:

$$V_n = \frac{f\left[e^{(n+1)\gamma\tau}(1+f)^{n+1} - 1\right]u\gamma - \left(e^{\gamma\tau} - 1\right)\left[e^{n\gamma\tau}(1+f)^n - 1\right]g}{e^{n\gamma\tau}(1+f)^n\left[e^{\gamma\tau}\gamma(1+f) - 1\right]}, \tag{12}$$

$$H_n = \frac{f(1+f)A_n u\gamma - gB_n}{e^{n\gamma\tau}(1+f)^n\left[e^{\gamma\tau}(1+f) - 1\right]^2\gamma^2}, \tag{13}$$

with

$$A_n = -e^{\gamma\tau} + 1 + e^{n\gamma\tau}(1+f)^n\left\{1 + n + e^{2\gamma\tau}(1+f)n - e^{2\gamma\tau}\left[1 + (2+f)n\right]\right\},$$

$$\begin{aligned} B_n = {} & 1 + f - 2e^{\gamma\tau}(1+f) + e^{2\gamma\tau}(1+f) - \\ & - \left\{e^{n\gamma\tau}(1+f)^n\left[1 + f + fn - n\gamma\tau - e^{2\gamma\tau}(1+f)\left[-1 + n\gamma\tau + fn(-1+\gamma\tau)\right]\right.\right. \\ & \left.\left. - e^{\gamma\tau}\left[2 + f^{2n} - 2n\gamma\tau + f\left[2 + n(2-2\gamma\tau)\right]\right]\right]\right\}. \end{aligned}$$

The limit velocity is obtained as

$$V_{n\to\infty} = \frac{g(1-e^{\gamma\tau}) + e^{\gamma\tau}f(1+f)u\gamma}{\gamma\left[e^{\gamma\tau}(1+f) - 1\right]}, \tag{14}$$

As a check, in the limit of vanishing drag ($\gamma \to 0$), the limit velocity becomes

$$V_{\substack{n\to\infty \\ \gamma\to 0}} = u + fu - \frac{g\tau}{f}, \tag{15}$$

which is identical with the value obtained in [10] for the same problem but for the frictionless motion case.

The velocity and position as functions of time can be obtained by taking intervals of the form $\left[t/\tau\right]\tau \le t < \left(\left[t/\tau\right]+1\right)\tau$, where $\left[t/\tau\right]$ is the integer part of the ratio t/τ . Thus, similarly to Eq. (3a), we can write the velocity as

$$v(t)=\left(V_{[t/\tau]}+\frac{g}{\gamma}\right)e^{-\gamma\left(t-[t/\tau]\tau\right)}-\frac{g}{\gamma}. \tag{16}$$

For the position, we can write

$$h(t)=H_{[t/\tau]}+y_{[t/\tau]}, \tag{17}$$

where, similarly to Eq. (3b),

$$y_{[t/\tau]}=\frac{1}{\gamma}\left(V_{[t/\tau]}+\frac{g}{\gamma}\right)\left(1-e^{-\gamma\left(t-[t/\tau]\tau\right)}\right)-\frac{g\left(t-[t/\tau]\tau\right)}{\gamma}.$$

In the limit of vanishing drag ($\gamma\to 0$) one checks that both equation (16) and (17) pass into the form obtained in [10] valid for the frictionless motion case.

Next, we describe the characteristics of the kinematics as function of the parameters τ, *f*, *u*, and *g* as follows: (*a*) to permanently have velocity V_n directed against the gravitational field, we impose the condition $V_n(\tau)>0$; (*b*) to have a permanently increasing velocity V_n, we impose the condition $V_{n+1}(\tau)>V_n(\tau)$; (*c*) to have not a return of the PES to the starting position, we impose the condition $H_n(\tau)>0$ (and keep in mind that, after each pulse, the position with the respect to the origin can only increase); (*d*) to have a faster than linear increase of $H_n(\tau)$ with *n*, we require a positive second derivative of $H_n(\tau)$ as function of *n*, that is $H_{n+2}(\tau)-2H_{n+1}(\tau)+H_n(\tau)>0$. The maximum values of the solution for the inequalities (*a*) – (*d*), that we name critical periods, are presented in Table 1. The third column shows an equivalent expression of the inequality from the second column. As one can see, the check with the frictionless case for the value of the critical periods from Table 1 of [10] (denoted by a star superscript in the fourth column of Table 1 in the present paper) is passed. Differently from the frictionless case, for condition (*c*) only a numerical solution can be obtained in the presence of linear drag (and this gives the semi-analytical character to our results). However, as already mentioned, for the frictionless limit, the inequality (*c*) becomes analytic and its critical value is identical with the value from [10] (denoted τ_2^* by us).

3. APPLICATIONS OF THE THEORY TO SOME PARALARVA MOTION

In this section we apply the theory from the previous section to the motion of some jetting *paralarva* (JP) species of meso-plankton [14]. The main criterion which should be satisfied for a Stokes flow is that the Reynolds number (defined as the ratio of inertial forces to viscous forces, see, *e.g.*, [15]),

$$Re = \rho_f LV/\eta, \tag{18}$$

should be sub-unitary; ρ_f is density of the fluid, L is a characteristic linear dimension of the object, V is the speed of the object relative to the fluid, and η is the fluid viscosity. To obtain sub-unitary values for *Re*, we consider the following parameters for the motion of some squids in sea water: $\rho_f = 1025\ \text{kg/m}^3$, $\eta = 1.58\times10^{-3}\ \text{kg/(m}\cdot\text{s)}$ [16], the characteristic linear dimension (assimilated to the diameter of an assumed spherically shaped animal) $L = 0.46\ \text{mm}$ [14]. Another necessary ingredient in the modelling is the parameter γ. The Stokes force for a linear drag is [17]

$$F_s = 6\pi\eta rV = kV\ , \tag{19}$$

and consequently,

$$\gamma = \frac{k}{M} = \frac{6\pi\eta r}{M} = \frac{9\eta}{2\pi r^2\rho_s}, \tag{20}$$

where ρ_s is the JP (considered as a homogenous body) density. Numerically, considering ρ_s as 3% greater than that of sea water [13], we estimate $\gamma = 127.3\ \text{s}^{-1}$. The effective gravitational field intensity obtained as the resultant of weight and buoyancy (divided by mass) is $g = g_0(\rho_s - \rho_f)/\rho_s$, that is approximately $0.285\ \text{m/s}^2$ for the densities we mentioned and Earth's gravity field intensity approximated by $g_0 = 9.8\ \text{m/s}^2$. In the simulation we consider as reasonable values, $u = 0.085$ m/s and $f = 0.35$ [18]. With the numerical values we considered we obtain $\tau_1 = 0.0208$ s, $\tau_2 = 0.106$ s (after numerically solving the transcendental inequality (*c*) from Table 1). For this specific set of data τ_3 (recall that it represents the maximum time period necessary to permanently have velocity $V_n > 0$) does not exist, because the inequality $g > f(1+f)u\gamma$ from Table 1 (*a*) does not hold true. The ordering of the critical periods is similar to that in the frictionless case [10], that is $\tau_1 < \tau_2$. The initial velocity is $V_0 = fu = 0.02975$ m/s and the initial position (as we mentioned) is $H_0 = 0$ m. A period of order 0.1 s is close to the value of τ_2 reported by experiment [18]. Though $\tau_1 = 0.0208$ s is not a realistic period for JP, we consider this case given its mathematical relevance. Next, we present the results of simulation for the numerically values introduced above.

Table 1

Calulus of the critical periods

Ineq.	Equivalence of inequality	Solution of inequality	Solution of inequality when $\gamma \to 0$
(a)	$f_1(n)=\dfrac{fu\gamma}{g}\dfrac{(1+f)e^{\gamma\tau}-(1+f)^{-n}e^{-n\gamma\tau}}{(e^{\gamma\tau}-1)\left[1-e^{-n\gamma\tau}(1+f)^{-n}\right]}>1.$ $f_1(n)$ is decreasing with n.	$\lim\limits_{n\to\infty} f_1(n)>1 \Leftrightarrow \tau<\dfrac{1}{\gamma}\ln\dfrac{g}{g-f(1+f)u\gamma}$ and $g>f(1+f)u\gamma$.	$\tau<\dfrac{f(1+f)u}{g}=\tau_3^*.$
(b)	$f_2(n)=\dfrac{e^{-(n+1)\gamma\tau}(1+f)^{-n-1}\left(g-ge^{\gamma\tau}+fu\gamma\right)}{\gamma}>0.$	$\tau<\dfrac{1}{\gamma}\ln\dfrac{g+fu\gamma}{g}=\tau_1.$	$\tau<\dfrac{fu}{g}=\tau_1^*.$
(c)	$f_3(n)=\dfrac{A_n}{B_n}\dfrac{f(1+f)u\gamma}{g}>1.$	Transcendental inequality for τ ; its critical solution is denoted by τ_2.	$\tau<\dfrac{2f(1+f)u}{(2+f)g}=\tau_2^*.$
(d)	$f_4(n)=(e^{\gamma\tau}-1)(1+f)\dfrac{\left[e^{\gamma\tau}(1+f)\right]^{-n-2}\left[fu\gamma-g(e^{\gamma\tau}-1)\right]}{\gamma^2}>0.$	$\tau<\dfrac{1}{\gamma}\ln\dfrac{g+fu\gamma}{g}=\tau_1.$	$\tau<\dfrac{fu}{g}=\tau_1^*.$

In Fig. 1, the kinematic characteristics of the motion are shown. In accordance with relation (*a*) from Table 1, for $\tau = \tau_1$, the velocity at the end of each period is zero and it generally has a characteristic 'saw tooth' shape, instantaneously increasing after the pulse and then decreasing according to a combination of linear and exponential functions. The movement is similar to that in the frictionless case [10]. For $\tau = \tau_2$, JP shortly reaches the limit velocity during each period. In Fig. 1b, for $\tau = \tau_1$ the shape of the curve reminds the parabolic variation of position with time for the frictionless case [10]. The final position after each cycle in this case constantly increases with time. For $\tau = \tau_2$ in each cycle JP starts by jumping up from the axes origin and finishes by reaching the origin again as required by the inequality (*c*) in Table 1. As pictured in Fig. 1c for $\tau = \tau_1$ the value of the Reynolds number rapidly varies and takes values higher than unity most of the time. This indicates that for periods of τ_1 order the kinematics is only qualitatively described as the creeping (Stokes) flows is characterized by sub-unitary values of Re (see, *e.g.*, [19]). In comparison, for $\tau = \tau_2$ the Reynolds number is majority of the time (approximately 87% of period) sub-unitary and the kinematics description is more reliable in this case.

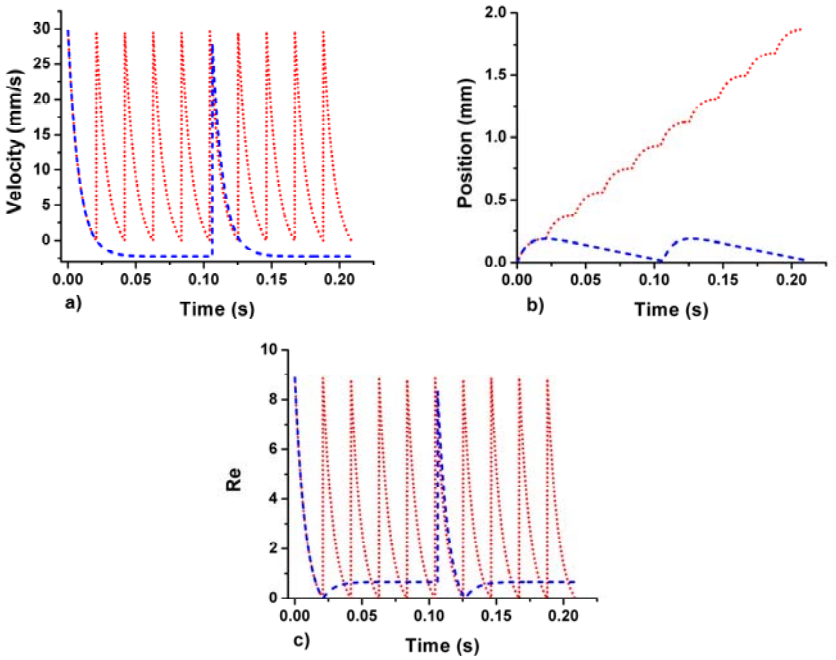

Fig. 1 – (Color online). Details of the motion: a) time variation of vertical velocity *v(t)* (obtained with Eq. (16)) for $\tau = \tau_1$ (red coloured dotted line) and for $\tau = \tau_2$ (blue coloured dashed line); b) time variation of the position *h*(*t*) (obtained with Eq. (17)): for $\tau = \tau_1$ (red coloured dotted line) and for $\tau = \tau_2$ (blue coloured dashed line); c) Re as a function of time (obtained with Eq. (18)) for $\tau = \tau_1$ (red coloured dotted line) and for $\tau = \tau_2$ (blue coloured dashed line).

Given that a realistic mantle contracting period is close to τ_2, the model can reasonably approximate the real motion of JP: the more powerful animals may maintain the altitude for a while by jumps as obtained in Fig. 1b [14, 18, 20].

For periods greater than τ_2 (in conformity with inequality (*c*) from Table 1) the JP eventually reaches positions below the starting point.

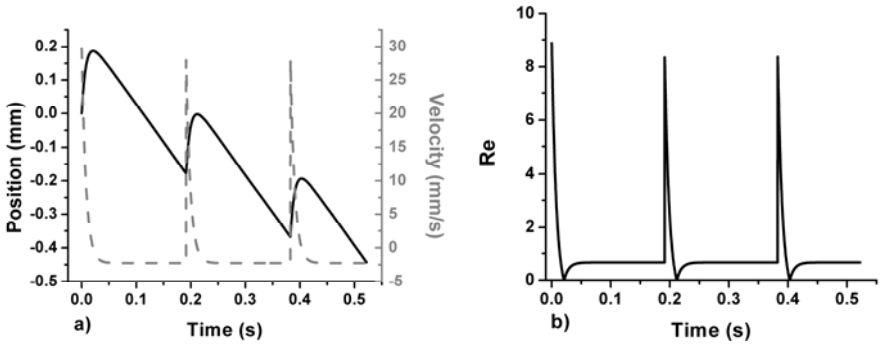

Fig. 2 – Details of the motion with $\tau = 1.8\tau_2$: a) the velocity *v(t)* (obtained with Eq. (16)) – grey dashed line and position *h(t)* (obtained with Eq. (17)) – black continuous line; b) Re as a function of time (obtained with Eq. (18)).

In Fig. 2 we analysed the case $\tau = 1.8\tau_2 = 0.1908$ s. The position at the end of each period is always below the starting point, since the velocity rapidly drops to a negative limit value. As one can see in Fig. 2b Re is majority of the time (approximately 92% of period) sub-unitary and this qualifies the kinematics description as reasonable. Such a motion corresponds to a less active JP which sank to the bottom with a speed of 5–20 mm/s similar to that reported by experiment [14, 18, 20].

4. CONCLUSIONS

In conclusion, by applying the momentum conservation we modelled the vertical dynamics of the PES in a uniform gravitational field with linear drag. The periodical motion reveals three critical values of the periods that define the characteristics of the motion. According to this finding, for period larger than a critical value τ_2 (see Table 1) the PES returns to the starting position. As a check, in the limit of frictionless motion we recover the results obtained in [10]. Regarding the accuracy of the model, generally, we find that the linear drag may be applied to a PES of small size of order 0.5 mm.

From pedagogical perspective, the power of the physics conservation laws in modelling the reality is emphasized. The PES dynamics is modelled by considering

the pulse as a pair of two perfect inelastic collision processes for the intake and exhaust. For PES of larger size, as for example, larger size squids, the modelling would require introducing a non-linear drag.

REFERENCES

1. S. Micluta-Câmpeanu and T.O. Cheche, Nonlinear Dyn. **89**, 81 (2017).
2. R. C. Stefan and T. O. Cheche, Rom. Rep. Phys. **69**, 904 (2017).
3. T.O. Cheche, Phys. Rev. B **73**, 113301 (2006).
4. T.O. Cheche, EPL **86**, 67011 (2009).
5. T.O. Cheche, V. Barna, and Y-C. Chang, Superlattices Microstruct. **60**, 475–486 (2013).
6. T.O. Cheche and M.C. Chang, Chem. Phys. Lett. **406**, 479–482 (2005).
7. C. Berlic and C. Miron, Rom. Rep. Phys. **69**, 120 (2017).
8. J. R. Dafler, Am. J. Phys **30**, 770 (1962).
9. R. Borghi and T. M. Spinozzi, Eur. J. Phys. **38**, 045006 (2017).
10. T.O. Cheche, Eur. J. Phys. **38**, 025001 (2017).
11. T.O. Cheche, Eur. J. Phys. **38**, 039502 (2017).
12. E. R. Trueman and A. Packard, J. Exp. Biol. **49**, 495 (1968).
13. W. Johnson, P. D. Soden, and E. R. Trueman, J. Exp. Biol **56**, 155 (1972).
14. R. Harris, P. Wiebe, J. Lenz, H. R. Skjoldal, and M. Huntley, *ICES Zooplankton Methodology Manual*, Academic Press, 2000.
15. R. B. Bird, W. E. Stewart, and E. N. Lightfoot, *Transport phenomena*, John Wiley & Sons, New York, 2002.
16. R. C. Weast, *CRC Handbook of Chemistry and Physics*, CRC Press, Ohio, 1968.
17. C. Collinson and T. Roper, *Particle Mechanics*, Elsevier, 2004.
18. I. K. Bartol, P. S. Krueger, J. T. Thompson, and W. J. Stewart, Integr. Comp. Biol. **48**, 720733 (2008).
19. B. Lautrup, *Physics of Continuous Matter Exotic and Everyday Phenomena in the Macroscopic World*, IOP Publishing Ltd, London, 2005, p. 271.
20. D.J. Staaf, S. Camarillo-Coop, S.H.D. Haddock, A.C. Nyack, J. Payne, C.A. Salinas-Zavala, B.A. Seibel, L. Trueblood, C. Widmer, and W.F. Gilly, J. Mar. Biol. Ass. UK **88** (4), 759 (2008).